NIH Public Access
Author Manuscript
J Photochem Photobiol B. Author manuscript; available in PMC 2011 December 2.

Published in final edited form as:
J Photochem Photobiol B. 2010 December 2; 101(3): 251–264. doi:10.1016/j.jphotobiol.2010.07.010.

The Malondialdehyde-derived Fluorophore DHP-lysine is a Potent Sensitizer of UVA-induced Photooxidative Stress in Human Skin Cells

Sarah D. Lamore[a], **Sara Azimian**[a], **David Horn**[a], **Bobbi L. Anglin**[a], **Koji Uchida**[b], **Christopher M. Cabello**[a], and **Georg T. Wondrak**[a,*]

[a] Department of Pharmacology and Toxicology, College of Pharmacy & Arizona Cancer Center University of Arizona Tucson, AZ, USA

[b] Graduate School of Bioagricultural Sciences, Nagoya University, Nagoya 464-8601, Japan

Abstract

Light-driven electron and energy transfer involving non-DNA skin chromophores as endogenous photosensitizers induces oxidative stress in UVA-exposed human skin, a process relevant to photoaging and photocarcinogenesis. Malondialdehyde is an electrophilic dicarbonyl-species derived from membrane lipid peroxidation. Here we present experimental evidence suggesting that the malondialdehyde-derived protein epitope dihydropyridine (DHP)-lysine is a potent endogenous UVA-photosensitizer of human skin cells. Immunohistochemical analysis revealed the abundant occurrence of malondialdehyde-derived and DHP-lysine epitopes in human skin. Using the chemically protected dihydropyridine-derivative (2S)-Boc-2-amino-6-(3,5-diformyl-4-methyl-4H-pyridin-1-yl)-hexanoic acid-t-butylester as a model of peptide-bound DHP-lysine, photodynamic inhibition of proliferation and induction of cell death were observed in human skin Hs27 fibroblasts as well as primary and HaCaT keratinocytes exposed to the combined action of UVA and DHP-lysine. DHP-lysine photosensitization induced intracellular oxidative stress, p38 MAP kinase activation, and upregulation of heme oxygenase-1 expression. Consistent with UVA-driven ROS formation from DHP-lysine, formation of superoxide, hydrogen peroxide, and singlet oxygen was detected in chemical assays, but little protection was achieved using SOD or catalase during cellular photosensitization. In contrast, inclusion of NaN_3 completely abolished DHP-photosensitization. Taken together, these data demonstrate photodynamic activity of DHP-lysine and support the hypothesis that malondialdehyde-derived protein-epitopes may function as endogenous sensitizers of UVA-induced oxidative stress in human skin.

Keywords

photosensitization; UVA; lipid peroxidation; skin photooxidative stress; DHP-lysine

[*]Address correspondence to: Georg T. Wondrak, Ph.D., University of Arizona, Arizona Cancer Center, 1515 North Campbell Avenue, Tucson, AZ 85724 USA, wondrak@pharmacy.arizona.edu, Telephone: 520-626-9017, Fax: 520-626-3979.

Publisher's Disclaimer: This is a PDF file of an unedited manuscript that has been accepted for publication. As a service to our customers we are providing this early version of the manuscript. The manuscript will undergo copyediting, typesetting, and review of the resulting proof before it is published in its final citable form. Please note that during the production process errors may be discovered which could affect the content, and all legal disclaimers that apply to the journal pertain.

NIH-PA Author Manuscript
NIH-PA Author Manuscript
NIH-PA Author Manuscript

NIH-PA Author Manuscript

NIH-PA Author Manuscript

NIH-PA Author Manuscript

1. Introduction

Light-driven electron and energy transfer involving non-DNA skin chromophores as endogenous photosensitizers is thought to contribute to oxidative stress in UVA-exposed human skin, a process with relevance to photoaging and photocarcinogenesis [1,2]. In contrast to the formation of mutagenic pyrimidine-base photoproducts through direct absorption of UVB (290 – 320 nm) radiation by skin cell DNA [3], UVA radiation results in little photoexcitation of DNA directly, and cutaneous generation of reactive oxygen species (ROS) and organic free radicals is now a widely accepted mechanism of UVA-phototoxicity (reviewed in [2,4–6]). In addition to various molecular sources including NAD(P)H oxidase and mitochondrial electron leakage that may contribute to cutaneous ROS formation in response to UV-exposure [7,8], a role of skin chromophores as endogenous sensitizers of photooxidative stress has been substantiated [1,2,9,10]. After initial formation of excited states of specific chromophores, photosensitization occurs as a consequence of their subsequent interaction with substrate molecules (type I photoreaction) or molecular oxygen (type II photoreaction) via energy and/or electron transfer [11]. In human skin, various chromophores including urocanic acid [12], riboflavin [13,14], B_6-vitamers [15], melanin precursors [16], and advanced glycation endproducts [17,18] have been proposed as endogenous UV-sensitizers, but molecular identity and causative involvement of relevant endogenous skin photosensitizers remain poorly understood [1,2,19–21].

Malondialdehyde (MDA) is an important reactive dialdehyde-intermediate resulting from lipid peroxidation chain reactions, and MDA has been involved in the pathogenesis of skin alterations associated with diabetes [22,23], nonmelanoma and melanoma skin cancer [24], and photoaging [25]. Tissue damage by lipid peroxidation-derived MDA involves covalent chemical adduction of protein-bound lysine residues potentially leading to fluorophore formation with protein crosslinking and further functional alterations [26–29]. Protein epitopes derived from MDA such as N^{ε}-(2-propenal)lysine (N-propenal-Lys) and dihydropyridine (DHP)-type adducts including DHP-lysine [(*S*)-2-amino-6-(3,5-diformyl-4-methyl-4H-pyridin-1-yl)-hexanoic acid; Fig. 1] may accumulate under conditions of chronic oxidative stress in damaged human tissue [27,30], and immunohistochemical analysis has identified DHP-lysine epitopes in cardiovascular atherosclerotic lesions [31]. Moreover, accumulation of MDA-derived epitopes with undefined chemical structure has been detected in cutaneaous superficial spreading melanoma and squamous cell carcinoma [24]. These epitopes are also thought to be major fluorophores contained in the intracellular age pigment lipofuscin that accumulates in lysosomes as a consequence of cumulative oxidative damage [32–35]. Importantly, potential phototoxicity of lipofuscin has been demonstrated in the context of age-related macular degeneration where accumulation of the all-trans-retinal derived lipofuscin-fluorophore A2E induces blue light-dependent photooxidative stress in human retinal pigment epithelial cells [36]. In contrast, little is known about the potential phototoxicity of lipid peroxidation-derived protein epitopes in human skin.

In this study, we (*I*) demonstrate that MDA- and DHP-epitopes occur abundantly in healthy human skin and (*II*) provide experimental evidence suggesting that peptide-bound DHP-lysine is a potent sensitizer of UVA-induced photooxidative stress in cultured human skin cells.

2. Materials and methods

2.1. Chemicals

Protected DHP-lysine [(2S)-Boc-2-amino-6-(3,5-diformyl-4-methyl-4H-pyridin-1-yl)-hexanoic acid t-butyl ester] was purchased from NeoMPS (San Diego, CA). Identity of the preparation employed in sensitization experiments was confirmed by fluorescence

NIH-PA Author Manuscript

NIH-PA Author Manuscript

NIH-PA Author Manuscript

spectroscopy (Fig. 1) and electrospray mass spectrometry [ESI-MS; m/z 437.56, $(M+H)^+$] using a LCQ Classic quadrupole ion trap mass spectrometer from Thermo Finnigan (San Jose, CA). All other chemicals were from Sigma Chemical Co. (St. Louis, MO).

2.2 Irradiation with solar UVA

A KW large area light source solar simulator, model 91293, from Oriel Corporation (Stratford, CT) was used, equipped with a 1000 W Xenon arc lamp power supply, model 68920, and a VIS-IR bandpass blocking filter plus UVB and C blocking filter (output 320–400 nm plus residual 650–800 nm, for UVA). The output was quantified using a dosimeter from International Light Inc. (Newburyport, MA), model IL1700, with a SED033 detector for UVA (range 315–390 nm, peak 365 nm), at a distance of 365 mm from the source, which was used for all experiments. Using UVB/C blocking filter, the dose at 365 mm from the source was 5.39 mJ cm^{-2} sec^{-1} UVA radiation with a residual UVB dose of 3.16 μJ cm^{-2} sec^{-1}.

2.3. Cell culture

Dermal neonatal foreskin Hs27 fibroblasts from ATCC and human immortalized HaCaT keratinocytes were cultured in DMEM containing 10% fetal bovine serum [37]. Primary human epidermal keratinocytes (neonatal HEKn-APF, from Cascade Biologics, Portland, OR, USA) were cultured using Epilife medium supplemented with EDGS growth supplement. Cells were passaged using recombinant trypsin/EDTA and defined trypsin inhibitor. Cells were maintained at 37 °C in 5% CO_2, 95% air in a humidified incubator.

2.4. Immunohistochemical detection of cutaneous MDA- and DHP-lysine epitopes using a tissue microarray (TMA)

Triplicates of a commercial human skin TMA (NS21-01-TMA, age grouped female normal skin tissue array; specimens of undisclosed anatomical location; twenty four array dots derived from 12 individual donors; Cybrdi, Rockville, MD) were processed for H&E staining, pan-MDA-immunohistochemistry, and DHP-lysine immunohistochemistry, respectively. Immunohistochemistry was performed using the Discovery XT automated staining platform (VMSI, Ventana Medical Systems, Tucson, AZ). Deparaffinization and antigen retrieval of cells and tissue were performed online. All steps were perform on this instrument using VMSI validated reagents, including deparaffinization, cell conditioning (antigen retrieval with a borate-EDTA buffer), primary antibody staining, detection and amplification using a biotinylated-streptavidin-HRP and DAB (3,3′-diaminobenzidine tetrahydrochloride) system, and hematoxylin counterstaining. DHP-lysine-adducted proteins were visualized using a validated murine primary monoclonal antibody (1F83, provided by Koji Uchida, Nagoya University, Japan; dilution: 1:100) [31]. MDA-adducted proteins were visualized using a polyclonal rabbit anti-MDA antiserum (AP050), Biotrend-usa, Destin, FL; dilution: 1:50] [24]. Images were captured using an Olympus BX50 and Spot (Model 2.3.0) camera. Images were standardized for light intensity.

2.5. Assay for photosensitized inhibition of skin cell proliferation

Cells were seeded at 10,000 cells per dish on 35mm dishes. After 24 h, cells were washed, placed in PBS, and exposed to the combined or isolated action of photodynamic test compound and irradiation (UVA). After irradiation cells were washed and fresh culture medium was added. For exposure of unirradiated cells to preirradiated test compound (‘preirradiation exposure’; Fig. 8C), cells were first washed with PBS and then incubated for 30 min with DHP-lysine in PBS that had been UVA-exposed immediately before. Cell number was determined 72 hr later, and proliferation was compared to cells that received mock-irradiation in PBS.

NIH-PA Author Manuscript

NIH-PA Author Manuscript

NIH-PA Author Manuscript

2.6. Cell cycle analysis

Analysis occurred according to a published standard procedure [15]. Cells were seeded at 1 × 10^5 per dish on 35mm culture dishes (Sarstedt, USA) and left overnight to attach. After irradiation in the presence or absence of test compound, cells were washed with PBS and fresh culture medium was added. After 48 h cells were harvested by trypsinization, resuspended in 200 μl PBS, and placed on ice. After addition of 2 ml 70% (v/v) ethanol, 30% (v/v) PBS, cells were incubated for 30 min on ice. The fixed cells were pelleted by centrifugation, resuspended in 800 μl PBS, 100 μl ribonuclease A (1mg/ml PBS), and 100 μl propidium iodide (400 μg/ml PBS), and incubated for 30 min in the dark at 37°C. Cellular DNA content was determined by flow cytometry using the ModFit LT software, version 3.0 (Verity, Topsham, ME).

2.7. Flow cytometric analysis of cell viability

Induction of cell death was confirmed by annexin-V-FITC/propidium iodide (PI) dual staining of cells followed by flow cytometric analysis [15]. Cells (100,000) were seeded on 35 mm dishes and received photosensitization 24 hours later. For exposure of unirradiated cells to preirradiated test compound (‘preirradiation exposure’; Fig. 4C and G), cells were first washed with PBS and then incubated for 30 min with test compound in PBS that had been UVA-exposed immediately before. Cells were harvested 24 h after treatment and cell staining was performed using an apoptosis detection kit according to the manufacturer’s specifications (APO-AF, Sigma, St. Louis, MO).

2.8. Caspase-3 activation assay

Treatment-induced caspase-3 activation was examined in Hs27 fibroblasts using a cleaved/activated caspase-3 (asp 175) antibody (Alexa Fluor 488 conjugate, Cell Signaling, Danvers, MA, USA) followed by flow cytometric analysis as published recently [38]. Briefly, cells were harvested 24h after treatment, resuspended in PBS and fixed in 1% formaldehyde. Cells were then permabilized using 90% methanol and resuspended in incubation buffer (PBS, 0.5% BSA). After rinsing by centrifugation, cells were resuspended in incubation buffer (90 μl) and cleaved caspase-3 antibody (10 μl) was added. After incubation (40 min) followed by rinsing and centrifugation in incubation buffer, cells were resuspended in PBS and analyzed by flow cytometry.

2.9. p38 MAPkinase Western analysis

Analysis occurred according to a published standard procedure [15]. One day before treatment, 100,000 Hs27 fibroblasts were seeded on 35 mm dishes. Cells were washed 24 h later with PBS, followed by addition of 1 mL PBS and exposure to increasing doses of UVA (up to 9.9 J/cm^2) in the absence or presence of DHP-lysine. After irradiation or mock-treatment, cells were incubated for 30 min (37 °C, 5% CO_2), then washed with PBS, lysed in 1x SDS-PAGE sample buffer (200 μl, 0.375 M Tris HCl pH 6.8, 50% glycerol, 10% SDS, 5% β-mercaptoethanol, 0.25% bromophenol blue), heated for 3 min at 95 °C, and placed on ice. Samples were separated by 12% SDS-PAGE followed by immediate transfer to polyvinylidene difluoride membranes (Immobilon, Millipore, Bedford, MA). Equal protein loading and transfer was examined by reversible Ponceau staining and the membrane was then used for p38 immunostaining using primary antibodies directed against total p38 (rabbit polyclonal, #9212, Cell Signaling, Danvers, MA) and phospho-p38 (Thr180/Tyr182; rabbit polyclonal, #9211).

2.10. Heme oxygenase-1 (HO-1) immunoblot analysis

Analysis occurred according to a published standard procedure [37]. One day before treatment 100,000 Hs27 fibroblasts were seeded on 35 mm dishes. Cells were washed 24 h

NIH-PA Author Manuscript

NIH-PA Author Manuscript

NIH-PA Author Manuscript

later with PBS, followed by addition of 1 mL PBS and exposure to increasing doses of UVA (up to 9.9 J/cm^2) in the absence or presence of DHP-lysine. After irradiation or mock-treatment, fresh medium was added, and cells were incubated for 24 h (37 ° C, 5% CO_2), then washed with PBS, lysed in 1x SDS-PAGE sample buffer and heated for 3 min at 95 °C. Samples were separated by 12% SDS-PAGE followed by immediate transfer to nitrocellulose membranes (Optitran, Whatman, Piscataway, NJ, USA). Rabbit anti-HO-1 polyclonal antibody (Stressgen Bioreagents, Ann Arbor, MI) was used (1:5000 in 5% milk-PBST; overnight at 4° C). HRP-conjugated goat anti-rabbit antibody (Jackson Immunological Research, West Grove, PA, USA) was used at 1:10,000 dilution followed by visualization using enhanced chemiluminescence detection reagents. Equal protein loading was examined by α-actin-detection [mouse anti-actin monoclonal antibody (Sigma) at 1:1,500 dilution].

2.11. Thiobarbituric acid reactive substances (TBARS) Assay

A standard procedure for the relative assessment of lipid peroxidation based on the photometric determination of thiobarbituric acid (TBA)-reactive material was followed using 1,3-diphenylthiobarbituric acid (DPTBA) for increased sensitivity [39]. One hour after photosensitization by exposure to the combined action of UVA and DHP-lysine HaCaT keratinocytes were harvested by trypsinization. Untreated control cells were equally processed. A pellet of 10×10^6 cells was then resuspended in 1.25 mL sodium acetate (330 mM, pH 3.0), mixed with 100 μL 1,3-diphenylthiobarbituric acid (DPTBA, 120 mM in DMSO), and heated (95 °C, 30 min). After cooling, the mixture was extracted with ethylacetate (0.6 mL), and the organic layer was used for relative photometric determination of TBARS by measuring absorbance at 538 nm on a Shimadzu spectrophotometer (model RF-540).

2.12. Detection of intracellular oxidative stress by flow cytometric analysis

Induction of intracellular oxidative stress by photosensitization was analyzed by flow cytometry using 2′,7′-dichlorodihydrofluorescein diacetate (DCFH-DA) as a sensitive non-fluorescent precursor dye according to a published standard procedure [38]. Human cultured skin cells were exposed to the isolated or combined action of UVA and DHP-lysine followed by DCFH-DA loading. To this end, 1 h after photosensitization cells were incubated for 1 h in the dark (37°C, 5% CO_2) with fresh culture medium containing DCFH-DA (5 μg/mL final concentration). Cells were then harvested, washed with PBS, resuspended in 300 μl PBS and immediately analyzed by flow cytometry. To avoid direct photooxidation of the dye probe, cells were first treated with UV irradiation and sensitizer and then loaded with the indicator dye under light exclusion.

2.13. Sensitization of protein photo-crosslinking and peptide photo-oxidation

Ribonuclease A (RNAse A, 10 mg/mL PBS) was irradiated (with UVA (9.9 J/cm^2) in the absence or presence of DHP-lysine (50 μM, 200 μL total reaction volume). Protein oligomerization as a result of sensitized photo-crosslinking was visualized by 15% SDS-PAGE followed by Coomassie-staining. Melittin (1 mg/mL PBS) was irradiated with UVA (9.9 J/cm^2) in the absence or presence of DHP-lysine (50 μM, 200 μL total reaction volume) followed by mass spectrometry.

2.14. Quantification of DHP-lysine sensitized superoxide formation

DHP-lysine sensitized generation of superoxide anions was determined by nitroblue tetrazolium chloride (NBT) reduction and confirmed by scavenging of superoxide by SOD [17]. A 200 μL reaction volume containing 0.8 μL of a NBT stock solution (50 mg/mL) and various concentrations of DHP-lysine was irradiated in the presence or absence of SOD

NIH-PA Author Manuscript

NIH-PA Author Manuscript

NIH-PA Author Manuscript

(3000 u) in triplicate on a 96 well microtiter plate. Replicate samples incubated in the dark were used as controls. Formation of nitroblue diformazan (NBF) as the photoreduction product was quantified measuring the absorbance at 560 nm on a Versamax microtiter plate reader (Molecular Devices, Sunnyvale, CA) using a nitroblue diformazan (NBF) standard curve.

2.15. Quantification of DHP-lysine sensitized hydrogen peroxide formation

DHP-lysine-sensitized-sensitized formation of peroxides was quantified according to a standard procedure with minor modifications [17]. Samples were prepared by UVA-irradiating DHP-lysine in PBS. Immediately after irradiation samples analyzed in triplicate on a 96 well microtiter plate. An aliquot (10 μl) was added to 95 μL H_2SO_4 (25 mM). After addition of 100 μl containing 0.5 mM ferrous ammonium sulfate, 200 μM xylenol orange, and 200 mM sorbitol in 25 mM H_2SO_4 the plate was incubated at room temperature for 30 min and the absorbance was determined at 570 nm on a Versamax microtiter plate reader (Molecular Devices, Sunnyvale, CA). A standard curve was generated using H_2O_2 as standard. Optionally, to ensure specificity of the assay, replicate samples were irradiated in the presence of catalase (400 u/mL) and after protein removal using spin microdialysis the peroxide measurement suppressible by catalase was assigned to H_2O_2.

2.16. Assessment of singlet oxygen formation using the RNO-bleaching assay

Following a published procedure for the detection of singlet oxygen in aqueous solution, p-nitrosodimethylaniline (RNO, 5 μM final concentration), Rose Bengal (RB, 1 μM, final concentration), and imidazole (8 mM, final concentration) were dissolved in PBS, pH 7.2 [40]. To 200 μL of this stock solution 50 μL of DHP-lysine or Rose Bengal dissolved in PBS at various concentrations (1–50 μM) were added and the final mixture was placed on a 96 well microtiter plate and subsequently exposed to increasing doses of UVA. In the assay solution, the reaction between imidazole and singlet oxygen results in the formation of a transannular peroxide that can bleach RNO. Loss of initial RNO absorbance due to singlet oxygen-dependent bleaching was monitored at 438 nm using a Versamax microtiter plate reader (Molecular Devices, Sunnyvale, CA). Duplicate samples were irradiated in the presence of the quencher NaN_3 (10 mM) in order to substantiate singlet oxygen involvement in DHP-lysine- or Rose Bengal-dependent RNO bleaching.

2.17. Peptide Mass spectrometry

Mass spectrometry was performed using a Bruker Reflex III MALDI–TOF-Mass Spectrometer (MALDI-TOF-MS) equipped with a nitrogen laser (337 nm). Spectra were recorded in positive ion mode in linear configuration using α-cyano-4-hydroxycinnamic acid as matrix.

2.18. Spectroscopy

UV-spectra were recorded using a Cary 100 Bio UV-Visible Spectrophotometer from Varian, Inc. (Palo Alto, CA). Fluorescence spectra were recorded using a Spectramax Gemini XS (Molecular Devices, Sunnyvale, CA) 96 well-microtiter plate reader.

2.19. Statistical analysis

The results are presented as means (+ SD) of at least three independent experiments. All data were analyzed employing *one-way* analysis of variance (*ANOVA)* with Tukey's *post hoc* test using the Prism 4.0 software. Differences were considered significant at $p < 0.05$. In all bar graphs, means with common letter differ ($p<0.05$).

NIH-PA Author Manuscript

NIH-PA Author Manuscript

NIH-PA Author Manuscript

3. Results

3.1. MDA- and DHP-epitopes occur in healthy human skin

First, cutaneous occurrence of lipid peroxidation-derived MDA- and DHP-epitopes was examined by immunohistochemical analysis of healthy human skin samples derived from a commercial cutaneous tissue microarray (Fig. 2; three representative specimens derived from 12 individual donors are depicted). Every specimen was analyzed by H&E staining, immunostaining for pan-MDA-derived epitopes, and specific immunodetection of DHP-lysine epitopes. Abundant immunoreactivity for MDA- and DHP-epitopes was detected throughout the epidermal and dermal layers with intra and extracellular localization. Similar immunostaining was observed with all 12 human skin specimens (data not shown). Remarkably, immunostaining for MDA- and DHP-epitopes was detectable with highest intensity in the cellular epidermis, with somewhat attenuated staining throughout the dermis, and no immunoreactivity for either epitope was observed throughout the stratum corneum. Dermal staining for pan-MDA-epitopes occurred with higher intensity than for DHP-lysine epitopes.

3.2. DHP-lysine as a sensitizer of UVA-induced inhibition of skin cell proliferation

Next, we tested the hypothesis that the DHP-lysine epitope displays activity as an UVA photosensitizer. To this end, we used Boc-protected DHP-lysine-tert.-butylester (termed ‘DHP-lysine’ throughout the results part), a synthetically accessible analogue of peptide-bound DHP-lysine with identical fluorophore structure as detailed in Fig. 1B-C and ‘Materials and methods’.

Consistent with a photodynamic activity associated with the fluorophore DHP-lysine, proliferation of human immortalized HaCaT keratinocytes was strongly suppressed upon combined exposure to a dose range of UVA-radiation in the presence of low micromolar concentrations of DHP-lysine, whereas exposure to the single action of DHP-lysine (up to 10 μM) or UVA (up to 9.9 J/cm^2) did not inhibit cellular proliferation (Fig. 3A–B). Photodynamic effects on proliferation were observable at low concentrations of DHP-lysine (1 μM) requiring only a moderate dose of UVA (9.9 J/cm^2; Fig. 3A). Similarly, proliferation was suppressed by by more than 50 % when a low dose of UVA (1.65 J/cm^2) was combined with DHP-lysine at a higher concentration (10 μM; Fig. 3B). Antiproliferative effects on HaCaT keratinocytes were confirmed by flow cytometric cell cycle analysis that revealed significant accumulation of HaCaT cells in the G_2/M phase resulting from DHP-lysine photosensitization (4.95 J/cm^2 UVA; 10 μM DHP) but not from single treatment with UVA or DHP-lysine only (Fig. 3C). The pronounced accumulation of keratinocytes with 4n DNA content (27.7 + 3.4 %, 48h after photosensitization; 13.2 + 1.7 %, untreated controls) and depletion of cells with 2n DNA content (44.3 + 2.0 %, 48h after photosensitization; 56.2 + 3.2 %, untreated controls) is consistent with the sensitized induction of a G_2/M block.

Similarly, proliferation of human skin fibroblasts (Hs27) was antagonized by UVA/DHP-lysine cotreatment, performed at UVA doses and compound concentrations that did not impair proliferation if delivered as single treatment (Fig. 3D–E). Photosensitized inhibition of Hs27 cell proliferation occurred in a similar range of DHP-lysine concentrations and UVA doses as observed with HaCaT keratinocytes.

3.3. DHP-lysine as a sensitizer of UVA-induced skin cell death

Photodynamic induction of skin cell death by UVA/DHP-lysine cotreatment was then examined by flow cytometric analysis of annexinV/PI-stained cells performed 24 h after treatment (Fig. 4). Viability of HaCaT keratinocytes exposed to the combined action of high concentrations of DHP-lysine (50 μM) and UVA (9.9 J/cm^2) was strongly reduced (Fig.

NIH-PA Author Manuscript

NIH-PA Author Manuscript

NIH-PA Author Manuscript

4A). An even more pronounced reduction in cell viability as a result of coexposure to DHP-lysine and UVA was observed in primary human epidermal keratinocytes (HEK) that displayed increased sensitivity to photodynamic induction of cell death as compared to HaCaT keratinocytes (Fig. 4D). Cell death of HaCaT keratinocytes occurred independent of caspase-activation since viability was not maintained if photodynamic treatment occurred after pre-exposure to zVADfmk, a potent pan-caspase inhibitor known to block caspase-dependent cell death (Fig. 4B) [38]. Interestingly, cell viability was completely unaffected if unirradiated cells were exposed to DHP-lysine (50 μM) that had been pre-exposed to UVA (9.9 J/cm^2) as specified in 'Materials and methods' suggesting that photodynamic induction of HaCaT cell death depends on the formation of a short-lived cytotoxic factor that is absent from the pre-irradiated DHP-lysine preparation (Fig. 4C).

Similarly, viability of human Hs27 skin fibroblasts was strongly impaired by UVA/DHP-lysine cotreatment performed at high UVA doses and compound concentrations that did not impair viability if delivered as single treatment (Fig. 4E). Upon combined exposure to DHP-lysine (50 μM) and UVA (9.9 J/cm^2) no viable cell population was detectable by flow cytometry (Fig. 4E). Pronounced activation of caspase 3 as evident from flow cytometric detection of proteolytically cleaved procaspase 3 could be detected in Hs27 fibroblasts only in response to exposure to the combined action of DHP-lysine and UVA (Fig. 4G). However, as seen with HaCaT keratinocytes, no protection from photodynamic induction of cell death was achieved by pan-caspase inhibition (Fig. 4F) suggesting that necrotic cell death occurred independent of caspase activation. Indeed, upon microscopic inspection immediately after irradiation, cell morphology had changed dramatically displaying extensive rounding and vacuolarization consistent with necrosis. As observed with HaCaT keratinocytes, Hs27 cell viability was unaffected if unirradiated cells were exposed to preirradiated DHP-lysine (Fig. 4H).

3.4. Skin cell oxidative stress resulting from DHP-lysine photosensitization

To examine whether the observed cellular photosensitization by DHP-lysine is associated with induction of oxidative stress, generation of intracellular oxidizing species was examined after exposing HaCaT and Hs27 cells to UVA in the presence or absence of DHP-lysine followed by loading with the redox-indicator DCFH-DA (5A and C) thought to be irreversibly oxidized and converted to the fluorescent dye DCF. Exposure of keratinocytes (Fig. 5A) and fibroblasts (Fig. 5C) to UVA in the absence of sensitizer induced a small but significant increase (approximately 50%) over baseline fluorescence observed after loading the cells with the redox dye, which is consistent with UVA-induced intracellular oxidative stress [2]. Exposure to DHP-lysine alone did not induce any enhancement of baseline fluorescence. When cells were exposed to the combined action of UVA and DHP-lysine, an up to 4-fold additional increase of DCF-fluorescence intensity was observed. These data demonstrate that photosensitization of skin cells by DHP-lysine enhances intracellular oxidative stress with formation of reactive species of sufficient longevity, such as protein peroxides [41], capable of oxidizing DCFH during cell loading after irradiation. Consistent with DHP-lysine-induced photooxidative stress, lipid peroxidation as assessed by formation of TBARS was elevated three-fold over control levels in photosensitized HaCaT keratinocytes (Fig. 5B).

Activation of mitogen activated protein (MAP) kinases by phosphorylation is an established cellular response to photooxidative stress [42,43], and sensitizer-dependent potentiation of p38 activation by UVA has been used to assess photodynamic effectiveness of therapeutic and endogenous photosensitizers [15,44]. Using the combination of UVA and DHP-lysine, we investigated the photosensitized induction of p38–phosphorylation in cultured Hs27 skin cells (Fig. 5D). Cells were irradiated with increasing doses of UVA in the absence or presence of DHP-lysine and analyzed for p38-phosphorylation by Western blot analysis of

NIH-PA Author Manuscript

NIH-PA Author Manuscript

NIH-PA Author Manuscript

protein cell extracts prepared 30 min after irradiation. In Hs27 fibroblasts, UVA-induction of dual phosphorylation of p38 (Thr180/Tyr182) was greatly potentiated by DHP-lysine at UVA doses ≥ 3.3 J/cm^2. In addition, upregulation of cellular heme oxygenase I (HO-1) protein levels was examined as another established marker of UVA-associated photooxidative stress in skin fibroblasts [45]. Indeed, DHP-lysine/UVA cotreatment strongly upregulated cellular levels of HO-1 as revealed by Western immunodetection (Fig. 5E).

3.5. Peptide oxidation resulting from DHP-lysine-photosensitization

Cellular photosensitization is thought to be triggered by photooxidation of biological macromolecules [41,46]. Photosensitization of protein damage by DHP-lysine was examined using a ribonuclease A (RNAse A) photo-crosslinking assay. RNAse A was selected as a model target because it does not contain tryptophan residues, thereby excluding effects of this endogenous UV-sensitizer amino acid on photo-crosslinking [15]. When RNAse A (monomer, Mw 13,700 Da) was irradiated with UVA (9.9 J/cm^2) in the presence or absence of DHP-lysine (50 μM) covalent protein-dimerization (28,000 Da) was detected using reducing SDS-PAGE analysis (Fig. 6A). RNAse-dimerization occurred with an approximate yield of 5% as measured by gel densitometry (data not shown).

Sensitization of macromolecular damage by DHP-lysine was studied in more detail examining peptide photooxidation by MALDI-TOF mass spectrometry. The peptide melittin ($C_{131}H_{229}N_{39}O_{31}$, Mw 2845.97, monoisotopic peak), previously used as a model target in studies of peptide oxidation and radiation damage [47,48], was UVA-irradiated in the presence or absence of DHP-lysine (Fig 6B). UVA-irradiation of melittin in the absence of sensitizer did not induce the formation of any reaction products, but irradiation in the presence of DHP-lysine induced the formation of a reaction product in high yields. The detected mass increase of 32 u of the newly formed product [2877.76 u - 2845.80 u, monoisotopic peaks] provided clear evidence for DHP-lysine-sensitized introduction of molecular oxygen into the target peptide that could occur by type I or II photosensitization [41,48,49]. Remarkably, DHP-lysine dependent photooxidative modification of melittin was completely suppressed if UVA exposure occurred in the presence of the singlet oxygen quencher NaN_3. Consistent with mechanistic involvement of singlet oxygen in DHP-lysine dependent melittin photooxidation, the yield of photoproduct was increased by approximately 30 % (based on mass spectrometric peak intensity) when sensitization was performed in PBS prepared in D_2O, another independent probe for the mechanistic involvement of singlet oxygen (data not shown) [17]. In contrast, hydroxyl radical scavenging using mannitol, iron ion chelation using deferoxamine mesylate, scavenging of H_2O_2 and superoxide radical anion using catalase or superoxide dismutase, respectively, did not interfere with DHP-lysine sensitization of melittin photooxidation (data not shown).

3.6. Photosensitization of ROS formation by DHP-lysine

Next, direct chemical evidence for UVA-driven production of ROS from DHP-lysine was obtained. First, DHP-lysine-sensitized NBT reduction was examined as a function of DHP-lysine concentration (3.3 J/cm^2 UVA; Fig. 7A) or dose UVA (100 μM DHP; Fig.7B). In addition, the SOD-suppressible portion of photoreductively generated nitroblue diformazan (NBF) was determined serving as an established indicator of superoxide anion formation (Fig. 7B) [17]. At the highest UVA dose (3.3 J/cm^2) NBT photoreduction by DHP-lysine occurred with approximately equimolar stochiometry, e.g. UVA exposure of 80 μM DHP-lysine generated approximately 90 μM NBF (Fig.7A). Photoreductive generation of NBF was strongly inhibited in the presence of SOD, with more than 60% of NBF formation (100 μM DHP; 3.3 J/cm^2 UVA) blocked in the presence of SOD (15,000 u/mL).

NIH-PA Author Manuscript

NIH-PA Author Manuscript

NIH-PA Author Manuscript

Next, the dose response relationship of photosensitized H_2O_2 production was determined as a function of DHP-lysine concentration (Fig. 7C) and UVA dose (Fig. 7D). Significant production of H_2O_2 yielding concentrations up to 40 μM was observed only at high concentrations of DHP-lysine (50–800 μM) exposed to UVA (9.9 J/cm^2) (Fig. 7C). At the highest concentration DHP (800 μM) significant production of H_2O_2 was observed at UVA doses ≥ 3.3 J/cm^2 (Fig. 7D).

Generation of singlet oxygen during DHP-lysine photosensitization was examined using the RNO bleaching assay as described earlier (Fig. 7E) [40]. Rose Bengal, an established photosensitizer for the efficient photodynamic production of singlet oxygen upon exposure to UVA and visible light, was employed as a positive control. Inhibition of RNO bleaching by the singlet oxygen quencher NaN_3 was assessed in order to substantiate involvement of singlet oxygen in DHP-lysine/UVA-induced RNO bleaching. RNO bleaching by DHP-lysine photosensitization occurred as a function of DHP-lysine concentration (data not shown) and UVA dose (3.3 to 9.9 J/cm^2) and was strongly suppressed by inclusion of NaN_3 (Fig. 7D). The UVA dose response of RNO bleaching resulting from photosensitization by Rose Bengal (1 μM) was observed at a twenty fold higher concentration of DHP-lysine (20 μM), indicating an approximately twenty fold difference in the relative sensitizer potency of UVA-driven singlet oxygen production displayed by these two test compounds under the conditions employed.

3.7. Antioxidant suppression of DHP-lysine phototoxicity

After demonstrating UVA-induced phototoxicity of DHP-lysine associated with induction of oxidative stress in cultured human skin cells and chemical detection of ROS, feasibility of antioxidant protection against DHP-lysine phototoxicity was examined in Hs27 skin fibroblasts (Fig. 8). First, photodynamic induction of cell death was examined in the absence or presence of various antioxidants (Fig. 8A). Among various antioxidant agents tested, complete cytoprotection against photosensitized induction of cell death was observed when UVA exposure occurred in the presence of NaN_3. In contrast, no protection was observed upon cotreatment with catalase or SOD (data not shown). Similarly, inhibition of proliferation induced by combined treatment with UVA and DHP-lysine was strongly antagonized if photosensitization occurred in the presence of NaN_3, but catalase and NAC were not effective in protecting Hs27 cells (‘co-irradiation procedure’, Fig. 8B). However, when unirradiated cells were exposed to a high concentration of preirradiated DHP-lysine (50 μM; 9.9 J/cm^2 UVA; cells exposed immediately after UVA; ‘pre-irradiation exposure’), left on cells right after irradiation as detailed in “Materials and methods’, significant inhibition of proliferation was observed. This antiproliferative effect could be antagonized by performing cellular exposure to preirradiated DHP-lysine in the presence of catalase or NAC, but not in the presence of NaN_3 (Fig. 8C).

Taken together with the results obtained from chemical ROS assays (Fig. 7), these data strongly suggest that short-lived singlet oxygen is the dominant ROS that mediates cytotoxic effects of DHP-lysine if UVA-exposure occurs in the direct presence of target cells. However, if DHP-lysine photoactivation occurs in the absence of target cells singlet oxygen decay occurs before cells are exposed to the preirradiated material, and only the chemically stable ROS H_2O_2 formed with low efficiency from UVA-exposed DHP-lysine (Fig. 7C–D) is capable of inducing antiproliferative effects in unirradiated target cells.

4. Discussion

UVA-sensitization by cutaneous chromophores is an important mechanism of skin cell photooxidative stress contributing to photoaging and carcinogenesis [2]. Here we demonstrate that the lipid peroxidation-derived protein epitope DHP-lysine is contained in

NIH-PA Author Manuscript

NIH-PA Author Manuscript

NIH-PA Author Manuscript

human skin and present experimental evidence that DHP-lysine functions as a UVA-photosensitizer of cultured human skin cells.

Skin cell photosensitization by DHP-lysine resulted in dose dependent inhibition of proliferation, cell cycle arrest, and induction of cell death (Figs. 3 and 4). A causative involvement of oxidative mechanisms in skin cell phototoxicity of DHP-lysine was supported by detecting the sensitized formation of cellular peroxides and lipid peroxidation products (TBARS) (Fig. 5A–C). Moreover, UVA-induced upregulation of HO-1 expression and p38 MAPkinase-dependent stress signaling, established markers of photooxidative stress, were observed in skin fibroblasts (Fig. 5D–E) [42,43,50,51]. Chemical analysis revealed the light-driven formation of singlet oxygen, superoxide anion radicals, and hydrogen peroxide resulting from UVA exposure of DHP-lysine (Fig. 7).

Formation of singlet oxygen was the dominant causative factor underlying skin cell phototoxicity of DHP-lysine as suggested by (*I*) the dependence of photodynamic efficacy on irradiation of cells in the direct presence of the sensitizer (Fig. 4C and G), (*II*) protective efficacy of the singlet oxygen quencher NaN_3, not observed with other antioxidants including catalase and NAC (Fig. 8A), and (*III*) indirect chemical detection of singlet oxygen by determination of NaN_3-suppressible RNO bleaching that occurred at low concentrations of DHP-lysine (Fig. 7E). Moreover, DHP-lysine dependent melittin photooxidation was blocked by NaN_3 and enhanced by performing UVA exposure in D_2O (Fig. 6B). However, the mechanistic basis of DHP-lysine phototoxicity remains incompletely understood at this point, and the complex photochemistry involving type I and type II photosensitization mechanisms awaits further photochemical investigation. Future experiments will also examine the possibility that apart from UVA blue visible light may photoactivate DHP-lysine as suggested by its fluorescence excitation spectrum (Fig. 1C). Singlet oxygen-dependent modification of specific target proteins of cellular photosensitization has been described earlier [52, 53]. Although photosensitization of protein and peptide damage was demonstrated in simple chemical model systems in our experiments (Fig. 6), no specific protein targets involved in skin cell photosensitization by DHP-lysine have been identified at this point.

It is well established that lipid peroxidation-derived protein epitopes can originate from lysine adduction by reactive intermediates including MDA, 4-hydroxynonenal (4-HNE), and glyoxal that accumulate under conditions of oxidative stress in numerous damaged human tissues such as atherosclerotic lesions [27,31,54,55]. Consistent with the causative involvement of photooxidative stress in macromolecular chemical damage during skin photoaging and carcinogenesis [2,34,56,57], acrolein-, glyoxal, and 4-HNE-derived epitopes have been detected in photoaged skin [55,58]. Cutaneous abundance in MDA-epitopes of unresolved chemical structure has been observed earlier with pathological accumulation of these epitopes in superficially spreading melanoma and nonmelanoma skin cancer [24].

Our immunohistochemical analysis demonstrates for the first time the abundant occurrence of DHP-lysine epitopes on unknown target proteins in healthy human epidermis and dermis (Fig. 2). In this prototype IHC study using an age-grouped human skin TMA with cutaneous specimens of unspecified anatomical location, no attempt was made to correlate epitope abundance with chronological age or molecular markers of photoaging expressed in the skin specimen, an analysis to be performed and published elsewhere. Future experimentation will also involve identification of specific cutaneous intra- and extracellular target proteins modified by DHP-lysine, since earlier work has already demonstrated that chemical posttranslational modification of skin proteins through oxidation, glycoxidation, and amino-carbonyl reactions targets specific proteins including keratin [56], elastin [58], collagen [59], and vimentin [60]. It will also be interesting to compare photodynamic activity of free DHP-

NIH-PA Author Manuscript

NIH-PA Author Manuscript

NIH-PA Author Manuscript

lysine as performed in this study with DHP-lysine covalently incorporated into a defined peptide or protein structure.

DHP-lysine is an endogenous fluorophore associated with intracellular lipofuscin, a fluorescent age pigment known to accumulate in human fibroblasts under conditions of chronic oxidative stress [28,61]. Together with earlier findings that demonstrate detrimental effects of lipofuscin accumulation on cellular lysosomal and proteasomal function and redox homeostasis [35,62], our studies suggest a novel mechanistic role of lipofuscin-associated fluorophores as phototoxic mediators of skin photodamage as previously described for the lipofuscin-associated blue light fluorophore A2E involved in photooxidative deterioration of retinal pigment epithelial cells during progressive macular degeneration [36]. Future mechanistic studies will therefore test the hypothesis that MDA-derived DHP-lysine epitopes in skin may play a similar role as sensitizers of UVA-induced cutaneous oxidative stress. Given the established role of photosensitization reactions in the initiation of cellular lipid peroxidation reactions [63], and based on TBAR formation in DHP-lysine/UVA exposed keratinocytes (Fig. 5B), it is also tempting to speculate that UVA-activated MDA-derived protein-epitopes may cause further lipid peroxidation and cutaneous accumulation of additional sensitizing epitopes, a vicious cycle of skin photooxidative stress to be substantiated by future experiments.

Acknowledgments

Mass spectral analysis was performed by the University of Arizona, Department of Chemistry Mass Spectrometry Facility directed by Dr. Arpad Somogyi. Flow cytometric analysis was performed at the Arizona Cancer Center flow cytometry laboratory. Supported in part by grants from the National Institutes of Health [R01CA122484, ES007091, ES006694, Arizona Cancer Center Support Grant CA023074].

Abbreviations

CAT	catalase
DCFH-DA	2′,7′-dichlorodihydrofluorescein diacetate
DHP	dihydropyridine-lysine
DMEM	Dulbecco’s modified Eagle’s medium
ESI-MS	electrospray-ionization-mass spectrometry
FITC	fluorescein isothiocyanate
4-HNE	4-hydroxynonenal
HO-1	heme oxygenase 1
MALDI-TOF-MS	matrix assisted laser desorption-time of flight-mass spectrometry
MDA	malondialdehyde
NBF	nitroblue diformazan
NBT	nitroblue tetrazolium chloride
PI	propidium iodide
RB	Rose Bengal
RNAse A	ribonuclease A
RNO	p-nitrosodimethylaniline
ROS	reactive oxygen species

NIH-PA Author Manuscript

NIH-PA Author Manuscript

NIH-PA Author Manuscript

SOD	superoxide dismutase
TBARS	Thiobarbituric acid reactive substances
TMA	tissue microarray
UVA	ultraviolet A

References

1. Scharffetter-Kochanek K, Wlaschek M, Brenneisen P, Schauen M, Blaudschun R, Wenk J. UV-induced reactive oxygen species in photocarcinogenesis and photoaging. Biol Chem. 1997; 378:1247–1257. [PubMed: 9426184]
2. Wondrak GT, Jacobson MK, Jacobson EL. Endogenous UVA-photosensitizers: mediators of skin photodamage and novel targets for skin photoprotection. Photochem Photobiol Sci. 2006; 5:215–237. [PubMed: 16465308]
3. Brash DE, Rudolph JA, Simon JA, Lin A, McKenna GJ, Baden HP, Halperin AJ, Ponten J. A role for sunlight in skin cancer: UV-induced p53 mutations in squamous cell carcinoma. Proc Natl Acad Sci U S A. 1991; 88:10124–10128. [PubMed: 1946433]
4. Gasparro FP. Sunscreens, skin photobiology, and skin cancer: the need for UVA protection and evaluation of efficacy. Environ Health Perspect. 2000; 108(Suppl 1):71–78. [PubMed: 10698724]
5. Halliday GM. Inflammation, gene mutation and photoimmunosuppression in response to UVR-induced oxidative damage contributes to photocarcinogenesis. Mutat Res. 2005; 571:107–120. [PubMed: 15748642]
6. Cadet J, Douki T, Ravanat JL, Di Mascio P. Sensitized formation of oxidatively generated damage to cellular DNA by UVA radiation. Photochem Photobiol Sci. 2009; 8:903–911. [PubMed: 19582264]
7. Valencia A, Kochevar IE. Nox1-based NADPH oxidase is the major source of UVA-induced reactive oxygen species in human keratinocytes. J Invest Dermatol. 2008; 128:214–222. [PubMed: 17611574]
8. Salet C, Moreno G. Photodynamic action increases leakage of the mitochondrial electron transport chain. Int J Radiat Biol. 1995; 67:477–480. [PubMed: 7738412]
9. Kvam E, Tyrrell RM. Induction of oxidative DNA base damage in human skin cells by UV and near visible radiation. Carcinogenesis. 1997; 18:2379–2384. [PubMed: 9450485]
10. Dalle Carbonare M, Pathak MA. Skin photosensitizing agents and the role of reactive oxygen species in photoaging. J Photochem Photobiol B. 1992; 14:105–124. [PubMed: 1331386]
11. Foote CS. Definition of type I and type II photosensitized oxidation. Photochem Photobiol. 1991; 54:659. [PubMed: 1798741]
12. Menon EL, Morrison H. Formation of singlet oxygen by urocanic acid by UVA irradiation and some consequences thereof. Photochem Photobiol. 2002; 75:565–569. [PubMed: 12081316]
13. Sato K, Taguchi H, Maeda T, Minami H, Asada Y, Watanabe Y, Yoshikawa K. The primary cytotoxicity in ultraviolet-a-irradiated riboflavin solution is derived from hydrogen peroxide. J Invest Dermatol. 1995; 105:608–612. [PubMed: 7561167]
14. Baier J, Maisch T, Maier M, Engel E, Landthaler M, Baumler W. Singlet oxygen generation by UVA light exposure of endogenous photosensitizers. Biophys J. 2006; 91:1452–1459. [PubMed: 16751234]
15. Wondrak GT, Roberts MJ, Jacobson MK, Jacobson EL. 3-hydroxypyridine chromophores are endogenous sensitizers of photooxidative stress in human skin cells. J Biol Chem. 2004; 279:30009–30020. [PubMed: 15133022]
16. Kipp C, Young AR. The soluble eumelanin precursor 5,6-dihydroxyindole-2-carboxylic acid enhances oxidative damage in human keratinocyte DNA after UVA irradiation. Photochem Photobiol. 1999; 70:191–198. [PubMed: 10461458]
17. Wondrak GT, Jacobson EL, Jacobson MK. Photosensitization of DNA damage by glycated proteins. Photochem Photobiol Sci. 2002; 1:355–363. [PubMed: 12653475]

NIH-PA Author Manuscript

NIH-PA Author Manuscript

NIH-PA Author Manuscript

18. Wondrak GT, Roberts MJ, Jacobson MK, Jacobson EL. Photosensitized growth inhibition of cultured human skin cells: mechanism and suppression of oxidative stress from solar irradiation of glycated proteins. J Invest Dermatol. 2002; 119:489–498. [PubMed: 12190875]
19. Young AR. Chromophores in human skin. Phys Med Biol. 1997; 42:789–802. [PubMed: 9172259]
20. Heck DE, Vetrano AM, Mariano TM, Laskin JD. UVB light stimulates production of reactive oxygen species: unexpected role for catalase. J Biol Chem. 2003; 278:22432–22436. [PubMed: 12730222]
21. Wondrak GT, Jacobson MK, Jacobson EL. Identification of quenchers of photoexcited states as novel agents for skin photoprotection. J Pharmacol Exp Ther. 2005; 312:482–491. [PubMed: 15475591]
22. Slatter DA, Bolton CH, Bailey AJ. The importance of lipid-derived malondialdehyde in diabetes mellitus. Diabetologia. 2000; 43:550–557. [PubMed: 10855528]
23. Ye X, Tong Z, Dang Y, Tu Q, Weng Y, Liu J, Zhang Z. Effects of blood glucose fluctuation on skin biophysical properties, structure and antioxidant status in an animal model. Clin Exp Dermatol. 2010; 35:78–82. [PubMed: 19594769]
24. Sander CS, Hamm F, Elsner P, Thiele JJ. Oxidative stress in malignant melanoma and non-melanoma skin cancer. Br J Dermatol. 2003; 148:913–922. [PubMed: 12786821]
25. Yan SX, Hong XY, Hu Y, Liao KH. Tempol, one of nitroxides, is a novel ultraviolet-A1 radiation protector for human dermal fibroblasts. J Dermatol Sci. 2005; 37:137–143. [PubMed: 15734282]
26. Slatter DA, Murray M, Bailey AJ. Formation of a dihydropyridine derivative as a potential cross-link derived from malondialdehyde in physiological systems. FEBS Lett. 1998; 421:180–184. [PubMed: 9468302]
27. Del Rio D, Stewart AJ, Pellegrini N. A review of recent studies on malondialdehyde as toxic molecule and biological marker of oxidative stress. Nutr Metab Cardiovasc Dis. 2005; 15:316–328. [PubMed: 16054557]
28. Uchida K. Lipofuscin-like fluorophores originated from malondialdehyde. Free Radic Res. 2006; 40:1335–1338. [PubMed: 17090422]
29. Ishii T, Kumazawa S, Sakurai T, Nakayama T, Uchida K. Mass spectroscopic characterization of protein modification by malondialdehyde. Chem Res Toxicol. 2006; 19:122–129. [PubMed: 16411665]
30. Mahmoodi H, Hadley M, Chang YX, Draper HH. Increased formation and degradation of malondialdehyde-modified proteins under conditions of peroxidative stress. Lipids. 1995; 30:963–966. [PubMed: 8538386]
31. Yamada S, Kumazawa S, Ishii T, Nakayama T, Itakura K, Shibata N, Kobayashi M, Sakai K, Osawa T, Uchida K. Immunochemical detection of a lipofuscin-like fluorophore derived from malondialdehyde and lysine. J Lipid Res. 2001; 42:1187–1196. [PubMed: 11483619]
32. Terman A, Brunk UT. Oxidative stress, accumulation of biological ‘garbage’, and aging. Antioxid Redox Signal. 2006; 8:197–204. [PubMed: 16487053]
33. Kikugawa K, Ido Y. Studies on peroxidized lipids. V. Formation and characterization of 1,4-dihydropyridine- 3,5-dicarbaldehydes as model of fluorescent components in lipofuscin. Lipids. 1984; 19:600–608.
34. Widmer R, Ziaja I, Grune T. Protein oxidation and degradation during aging: role in skin aging and neurodegeneration. Free Radic Res. 2006; 40:1259–1268. [PubMed: 17090415]
35. Jung T, Bader N, Grune T. Lipofuscin: formation, distribution, and metabolic consequences. Ann N Y Acad Sci. 2007; 1119:97–111. [PubMed: 18056959]
36. Sparrow JR, Nakanishi K, Parish CA. The lipofuscin fluorophore A2E mediates blue light-induced damage to retinal pigmented epithelial cells. Invest Ophthalmol Vis Sci. 2000; 41:1981–1989. [PubMed: 10845625]
37. Wondrak GT, Cabello CM, Villeneuve NF, Zhang S, Ley S, Li Y, Sun Z, Zhang DD. Cinnamoyl-based Nrf2-activators targeting human skin cell photo-oxidative stress. Free Radic Biol Med. 2008; 45:385–395. [PubMed: 18482591]
38. Wondrak GT. NQO1-activated phenothiazinium redox cyclers for the targeted bioreductive induction of cancer cell apoptosis. Free Radic Biol Med. 2007; 43:178–190. [PubMed: 17603928]

NIH-PA Author Manuscript

NIH-PA Author Manuscript

NIH-PA Author Manuscript

39. Ohkawa H, Ohishi N, Yagi K. Assay for lipid peroxides in animal tissues by thiobarbituric acid reaction. Anal Biochem. 1979; 95:351–358. [PubMed: 36810]
40. Kraljic I, El Mohsni S. A new method for the detection of singlet oxygen in aqueous solutions. Photochem Photobiol. 1978; 28:577–581.
41. Wright A, Hawkins CL, Davies MJ. Photo-oxidation of cells generates long-lived intracellular protein peroxides. Free Radic Biol Med. 2003; 34:637–647. [PubMed: 12633741]
42. Bachelor MA, Bowden GT. UVA-mediated activation of signaling pathways involved in skin tumor promotion and progression. Semin Cancer Biol. 2004; 14:131–138. [PubMed: 15018897]
43. Klotz LO, Briviba K, Sies H. Mitogen-activated protein kinase activation by singlet oxygen and ultraviolet A. Methods Enzymol. 2000; 319:130–143. [PubMed: 10907506]
44. Buchczyk DP, Klotz LO, Lang K, Fritsch C, Sies H. High efficiency of 5-aminolevulinate-photodynamic treatment using UVA irradiation. Carcinogenesis. 2001; 22:879–883. [PubMed: 11375893]
45. Tyrrell RM. Solar ultraviolet A radiation: an oxidizing skin carcinogen that activates heme oxygenase-1. Antioxid Redox Signal. 2004; 6:835–840. [PubMed: 15345143]
46. Dolmans DE, Fukumura D, Jain RK. Photodynamic therapy for cancer. Nat Rev Cancer. 2003; 3:380–387. [PubMed: 12724736]
47. Guptasarma P, Balasubramanian D, Matsugo S, Saito I. Hydroxyl radical mediated damage to proteins, with special reference to the crystallins. Biochemistry. 1992; 31:4296–4303. [PubMed: 1567875]
48. Luxford C, Morin B, Dean RT, Davies MJ. Histone H1- and other protein- and amino acid-hydroperoxides can give rise to free radicals which oxidize DNA. Biochem J. 1999; 344:125–134. [PubMed: 10548542]
49. Davies MJ. Singlet oxygen-mediated damage to proteins and its consequences. Biochem Biophys Res Commun. 2003; 305:761–770. [PubMed: 12763058]
50. Camera E, Mastrofrancesco A, Fabbri C, Daubrawa F, Picardo M, Sies H, Stahl W. Astaxanthin, canthaxanthin and beta-carotene differently affect UVA-induced oxidative damage and expression of oxidative stress-responsive enzymes. Exp Dermatol. 2009; 18:222–231. [PubMed: 18803658]
51. Polte T, Tyrrell RM. Involvement of lipid peroxidation and organic peroxides in UVA-induced matrix metalloproteinase-1 expression. Free Radic Biol Med. 2004; 36:1566–1574. [PubMed: 15182858]
52. Davies MJ. Reactive species formed on proteins exposed to singlet oxygen. Photochem Photobiol Sci. 2004; 3:17–25. [PubMed: 14743273]
53. von Montfort C, Sharov VS, Metzger S, Schoneich C, Sies H, Klotz LO. Singlet oxygen inactivates protein tyrosine phosphatase-1B by oxidation of the active site cysteine. Biol Chem. 2006; 387:1399–1404. [PubMed: 17081112]
54. Fu MX, Requena JR, Jenkins AJ, Lyons TJ, Baynes JW, Thorpe SR. The advanced glycation end product, Nepsilon-(carboxymethyl)lysine, is a product of both lipid peroxidation and glycoxidation reactions. J Biol Chem. 1996; 271:9982–9986. [PubMed: 8626637]
55. Tanaka N, Tajima S, Ishibashi A, Uchida K, Shigematsu T. Immunohistochemical detection of lipid peroxidation products, protein- bound acrolein and 4-hydroxynonenal protein adducts, in actinic elastosis of photodamaged skin. Arch Dermatol Res. 2001; 293:363–367. [PubMed: 11550810]
56. Thiele JJ, Hsieh SN, Briviba K, Sies H. Protein oxidation in human stratum corneum: susceptibility of keratins to oxidation in vitro and presence of a keratin oxidation gradient in vivo. J Invest Dermatol. 1999; 113:335–339. [PubMed: 10469330]
57. Sander CS, Chang H, Salzmann S, Muller CS, Ekanayake-Mudiyanselage S, Elsner P, Thiele JJ. Photoaging is associated with protein oxidation in human skin in vivo. J Invest Dermatol. 2002; 118:618–625. [PubMed: 11918707]
58. Mizutari K, Ono T, Ikeda K, Kayashima K, Horiuchi S. Photo-enhanced modification of human skin elastin in actinic elastosis by N(epsilon)-(carboxymethyl)lysine, one of the glycoxidation products of the Maillard reaction. J Invest Dermatol. 1997; 108:797–802. [PubMed: 9129235]

NIH-PA Author Manuscript

NIH-PA Author Manuscript

NIH-PA Author Manuscript

59. Sell DR, Kleinman NR, Monnier VM. Longitudinal determination of skin collagen glycation and glycoxidation rates predicts early death in C57BL/6NNIA mice. Faseb J. 2000; 14:145–156. [PubMed: 10627289]

60. Kueper T, Grune T, Prahl S, Lenz H, Welge V, Biernoth T, Vogt Y, Muhr GM, Gaemlich A, Jung T, Boemke G, Elsasser HP, Wittern KP, Wenck H, Stab F, Blatt T. Vimentin is the specific target in skin glycation. Structural prerequisites, functional consequences, and role in skin aging. J Biol Chem. 2007; 282:23427–23436. [PubMed: 17567584]

61. Sitte N, Merker K, Grune T, von Zglinicki T. Lipofuscin accumulation in proliferating fibroblasts in vitro: an indicator of oxidative stress. Exp Gerontol. 2001; 36:475–486. [PubMed: 11250119]

62. Hohn A, Jung T, Grimm S, Grune T. Lipofuscin-bound iron is a major intracellular source of oxidants: role in senescent cells. Free Radic Biol Med. 2010; 48:1100–1108. [PubMed: 20116426]

63. Girotti AW. Photosensitized oxidation of membrane lipids: reaction pathways, cytotoxic effects, and cytoprotective mechanisms. J Photochem Photobiol B. 2001; 63:103–113. [PubMed: 11684457]

NIH-PA Author Manuscript

NIH-PA Author Manuscript

NIH-PA Author Manuscript

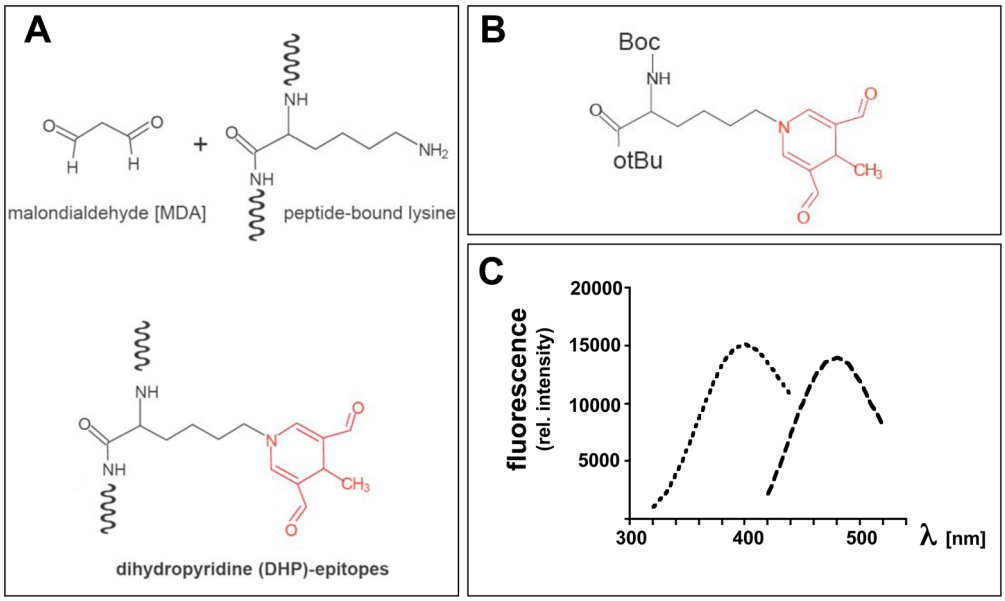

Figure 1. The lipid peroxidation-derived fluorophore dihydropyridine (DHP)-lysine

(A) Formation of DHP-epitopes on target lysine residues occurs by spontaneous malondialdehyde (MDA)-adduction. (B) Protected DHP-lysine as a model of peptide-bound DHP-lysine. (C) Fluorescence spectrum of protected DHP-lysine [excitation spectrum (λem at 485 nm; broken line, short dashes) and emission spectrum (λex at 395 nm; broken line, long dashes)]

NIH-PA Author Manuscript

NIH-PA Author Manuscript

NIH-PA Author Manuscript

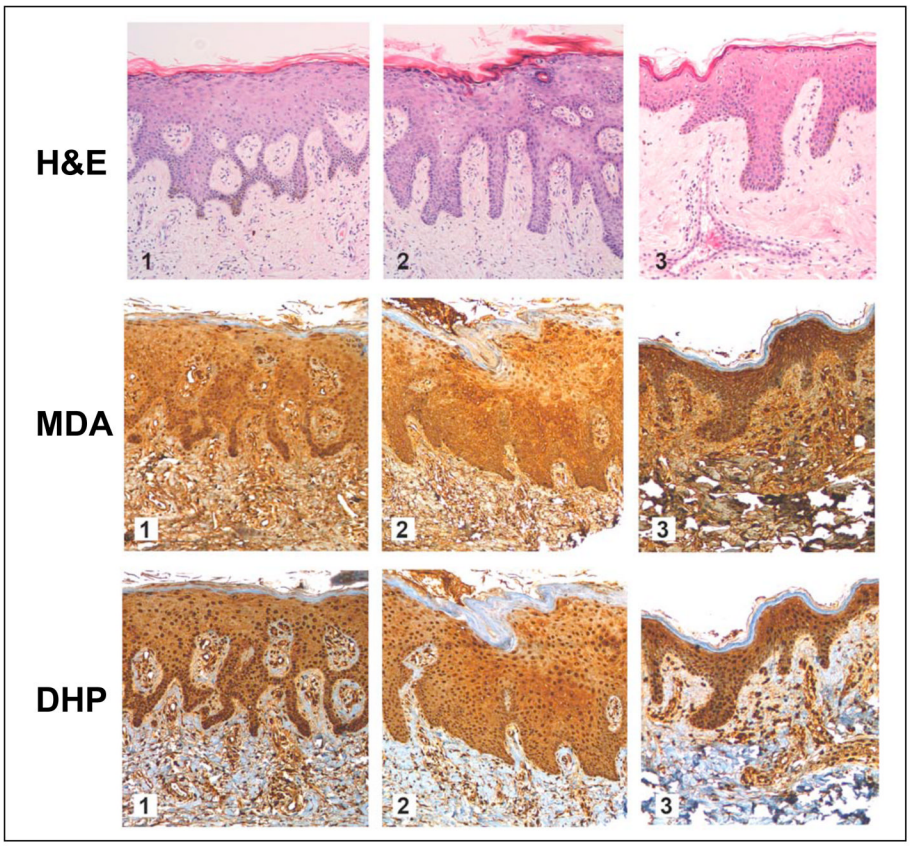

Figure 2. Immunohistochemical detection of MDA- and DHP-epitopes in healthy human skin

A commercially available healthy human skin tissue microarray (NS21-01-TMA, Cybrdi) was processed for H&E staining (top row, specimens 1–3), pan-MDA-immunohistochemistry (middle row, specimens 1–3) using a polyclonal antibody (AP050), and DHP-immunohistochemistry (bottom row, specimens 1–3) using a monoclonal antibody (1F83). In all specimens, abundant staining for MDA- and DHP-epitopes occurs throughout the epidermal and dermal layers; Staining is most abundant in the cellular layers of the epidermis. Stratum corneum does not stain positive for either epitope. Three representative specimens are depicted.

NIH-PA Author Manuscript

NIH-PA Author Manuscript

NIH-PA Author Manuscript

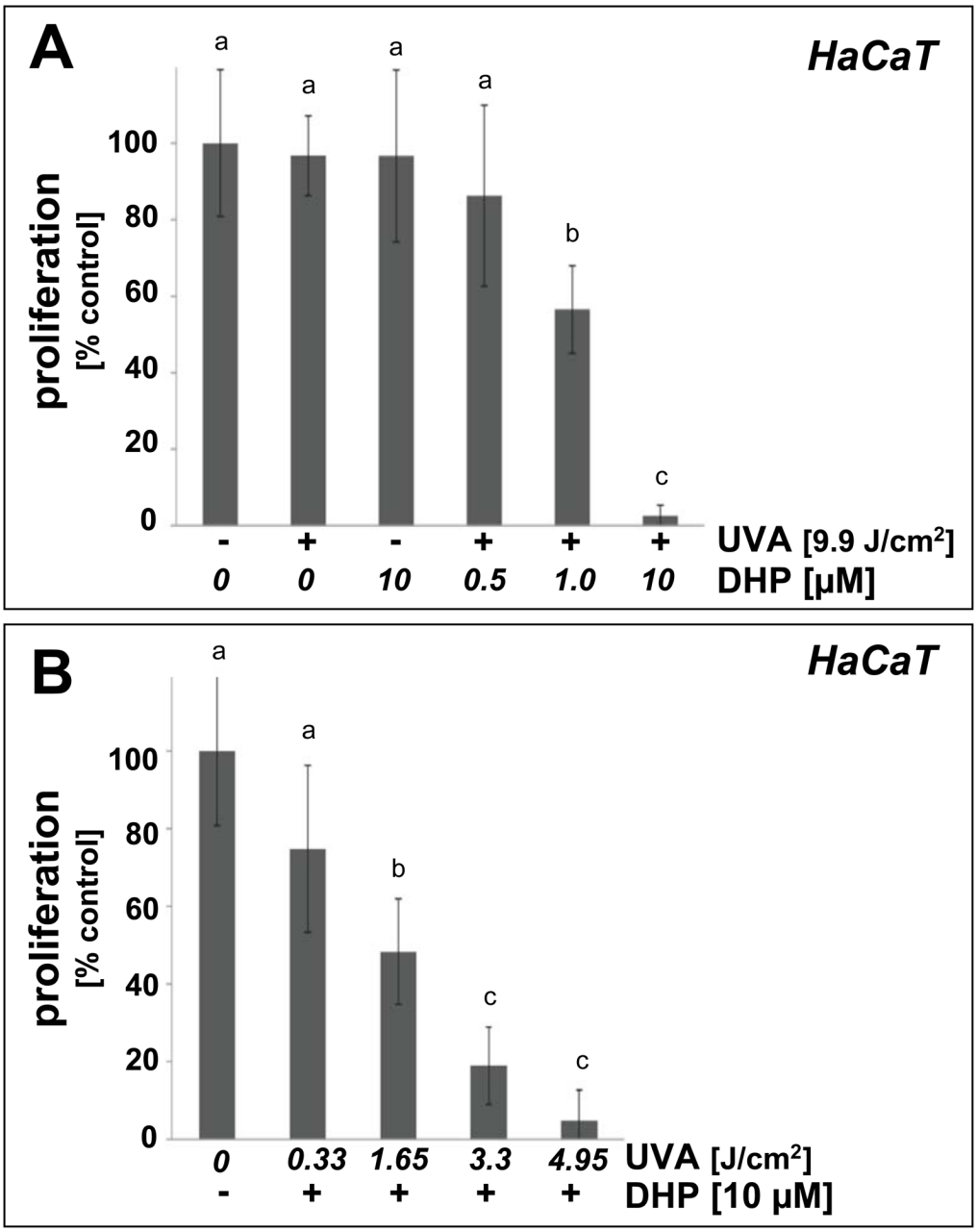

NIH-PA Author Manuscript

NIH-PA Author Manuscript

NIH-PA Author Manuscript

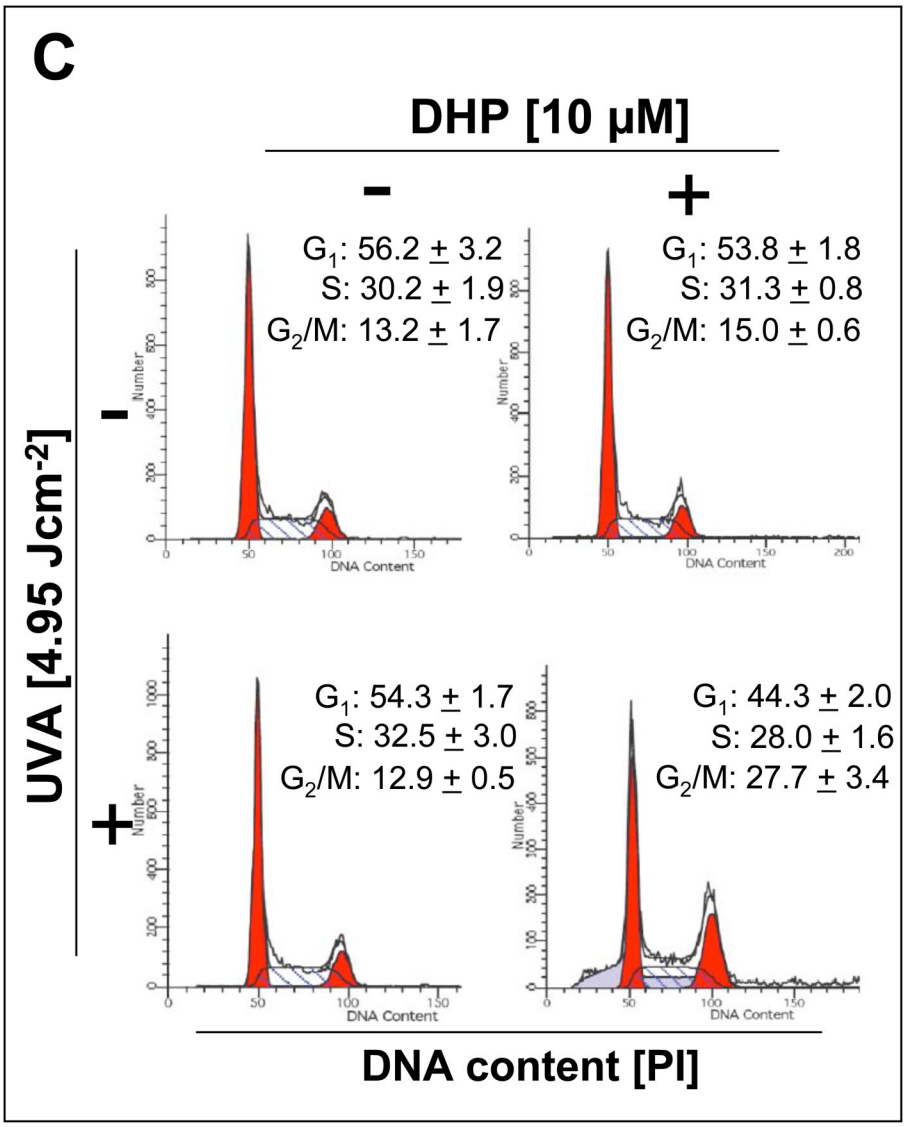

NIH-PA Author Manuscript

NIH-PA Author Manuscript

NIH-PA Author Manuscript

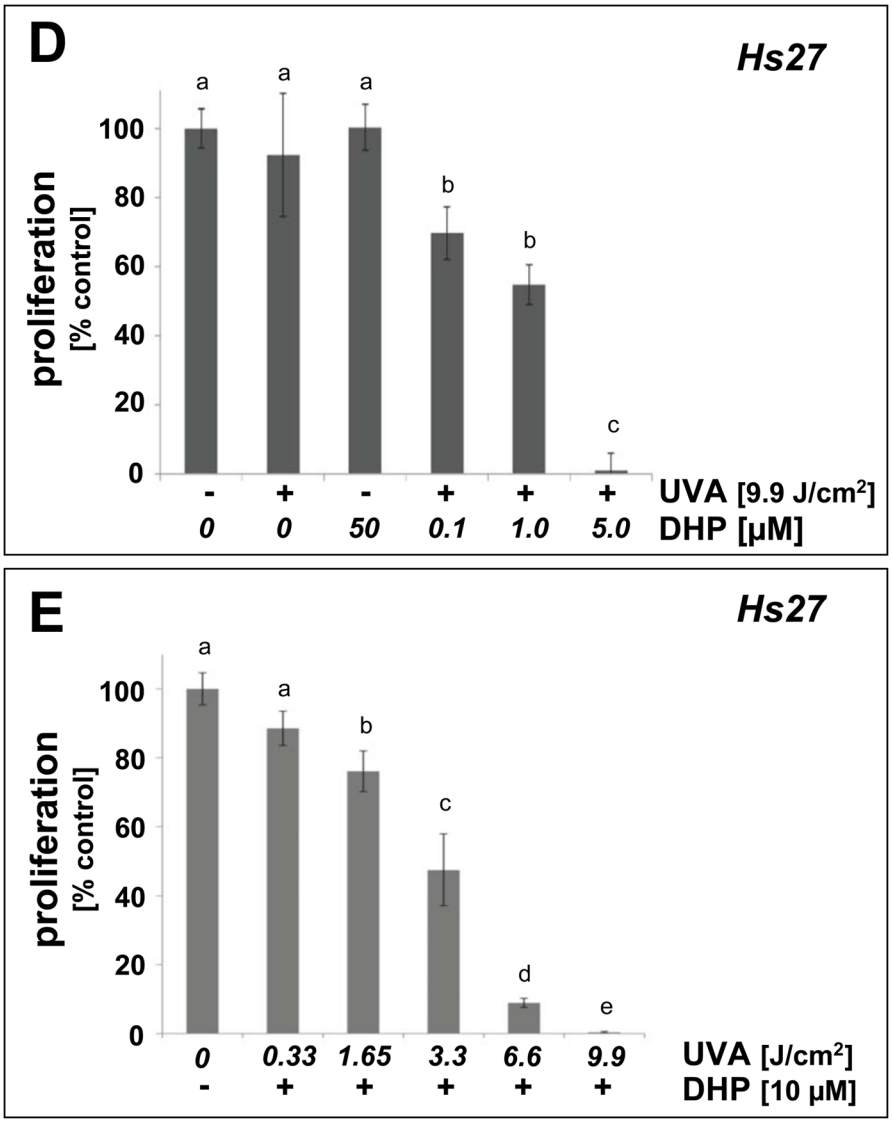

Figure 3. DHP-lysine as a photosensitizer of UVA-induced inhibition of skin cell proliferation

(A) Human immortalized HaCaT keratinocytes were exposed to UVA-irradiation (9.9 J/cm^2) in the presence or absence of DHP-lysine (0.5–10 μM). Additionally, mock-irradiated cells were exposed to DHP (10 μM). Cells were washed with PBS, fresh DMEM was added, and cell number was determined 72 h later by cell counting. Proliferation was compared to untreated cells. (B) HaCaT keratinocytes were exposed to increasing doses of UVA-irradiation (up to 4.95 J/cm^2) in the presence or absence of DHP-lysine (10 μM). Additionally, mock-irradiated cells were exposed to DHP (10 μM). After treatment, proliferation was assessed as detailed in panel A. (C) Cell cycle analysis by flow cytometric analysis of HaCaT keratinocytes stained with propidium iodide was performed 24h after photosensitization (DHP (10 μM); UVA (4.95 J/cm^2). Histograms of a representative experiment are shown. The numbers summarize results (% of total gated cells; mean + SD) from three independent experiments. (D–E) Human skin fibroblasts (Hs27) were exposed to UVA-irradiation in the presence or absence of DHP-lysine, and effects of photosensitization on proliferation were then examined as detailed in panels A–B. In the bar graphs, means with common letter differ ($p<0.05$).

NIH-PA Author Manuscript
NIH-PA Author Manuscript
NIH-PA Author Manuscript

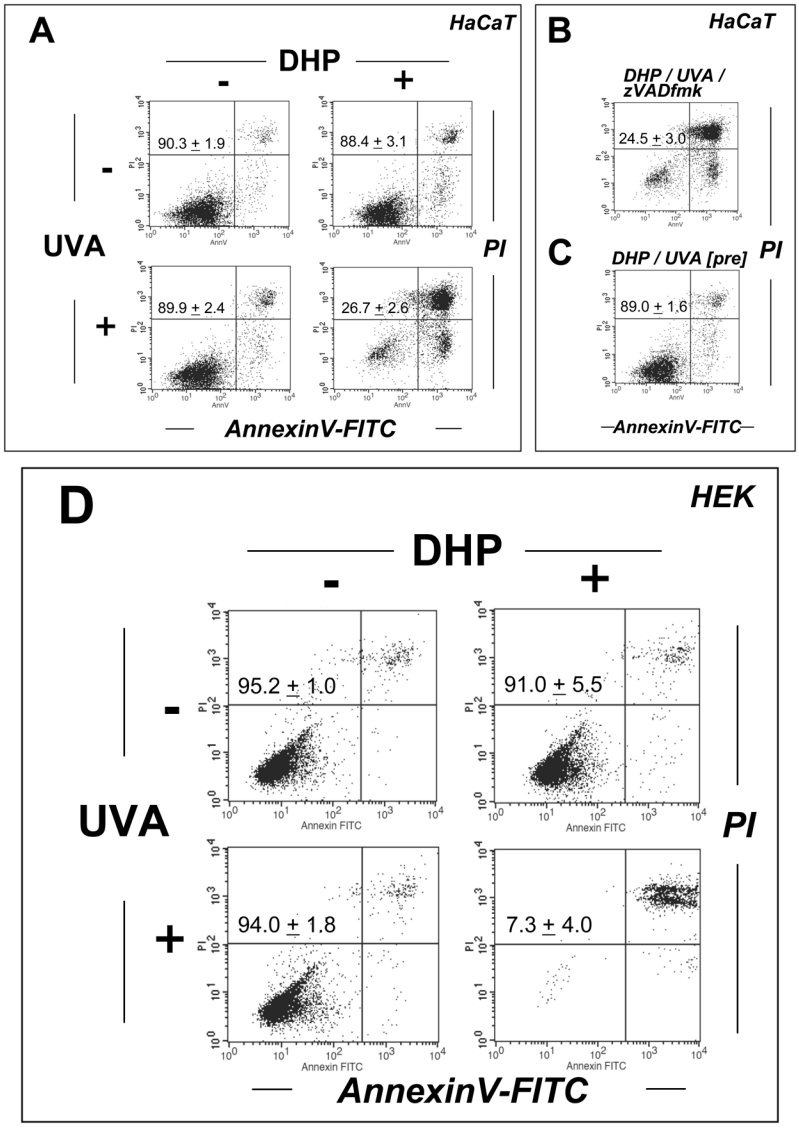

NIH-PA Author Manuscript

NIH-PA Author Manuscript

NIH-PA Author Manuscript

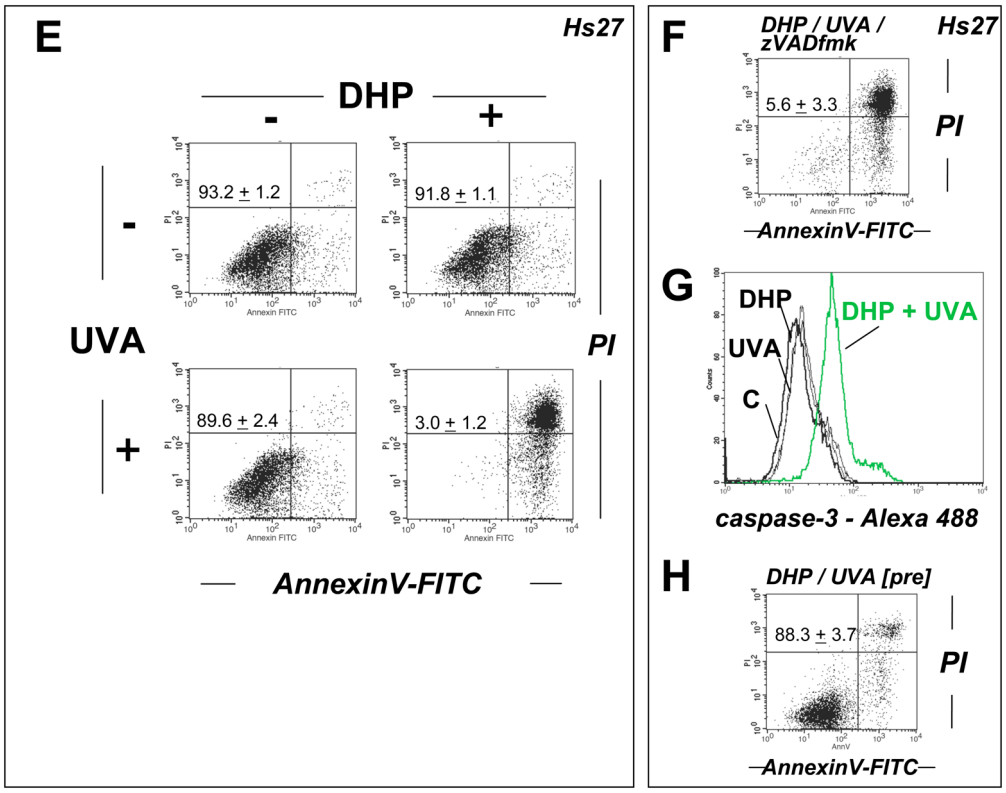

Figure 4. DHP-lysine as a photosensitizer of UVA-induced skin cell death

(A–C) HaCaT keratinocytes were exposed to the combined action of UVA irradiation (9.9 J/cm^2) and DHP-lysine (50 μM). (A) Induction of cell death 24 h after exposure was examined by flow cytometric analysis of annexinV-PI stained cells. (B) Photosensitization was performed as in panel A in the presence of zVADfmk. (C) Unirradiated cells were exposed to DHP (50 μM) that was UVA-preirradiated (9.9 J/cm2) and cell viability was examined 24 h after exposure. The numbers summarize results (% viable cells (lower left quadrant) of total gated cells; mean + SD) from three independent experiments. (D) Primary human epidermal keratinocytes (HEK) were exposed to the combined action of UVA irradiation (9.9 J/cm^2) and DHP-lysine (50 μM). Induction of cell death 24 h after exposure was examined by flow cytometric analysis of annexinV-PI stained cells. (E–H) Hs27 fibroblasts were exposed to the combined action of UVA irradiation (9.9 J/cm^2) and DHP-lysine (50 μM). (E) Induction of cell death 24 h after exposure was examined by flow cytometric analysis of annexinV-PI stained cells. (F) Photosensitization was performed as in panel A in the presence of zVADfmk. (G) Photosensitization was performed as in panel A, and caspase 3 activation was analyzed by flow cytometry using an Alexa 488-conjugated antibody directed against cleaved procaspase 3. (H) Unirradiated cells were exposed to DHP (50 μM) that was UVA-preirradiated (9.9 J/cm^2) and cell viability was examined 24 h after exposure. The numbers summarize results (% viable cells (lower left quadrant) of total gated cells; mean + SD) from three independent experiments.

NIH-PA Author Manuscript

NIH-PA Author Manuscript

NIH-PA Author Manuscript

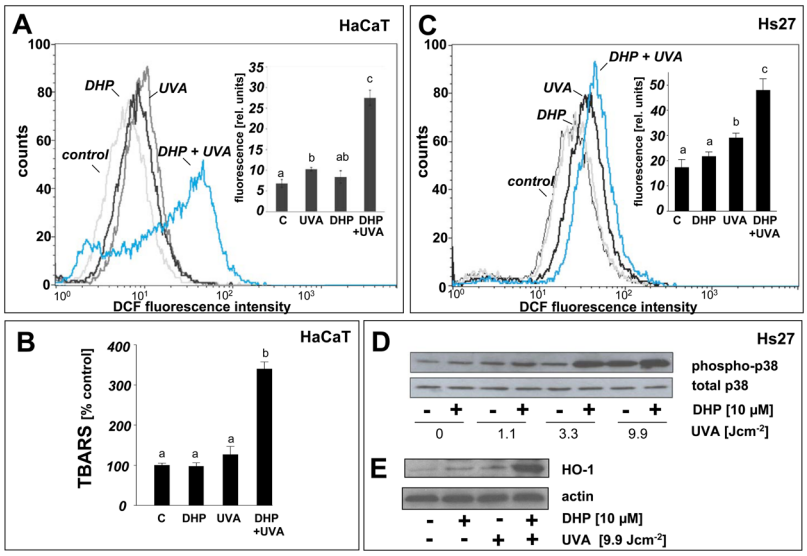

Figure 5. Induction of oxidative stress in cultured human skin cells resulting from DHP-lysine photosensitization

(A) HaCaT keratinocytes were exposed to UVA-irradiation (9.9 J/cm^2) in the presence or absence of DHP (50 μM) followed by loading with the intracellular redox dye DCFH-DA 1 h after irradiation. DCF-fluorescence intensity indicative of intracellular redox stress was then quantified by flow cytometric analysis. One representative histogram out of three similar repeats is shown. In the bar graph, means with common letter differ (n=3, mean + SD; $p<0.05$). (B) Lipid peroxidation resulting from DHP-lysine photosensitization was examined in HaCaT keratinocytes exposed as specified in (A) followed by photometric detection of TBARS. (C) Hs27 fibroblasts were exposed and analyzed as specified in (A). (D) Upregulation of cellular heme oxygenase-1 protein levels by the combined action of DHP-lysine and UVA was examined in Hs27 fibroblasts 24 h after photosensitization by Western blotting as described in Experimental Procedures. (E) Photosensitized induction of p38 MAPkinase phosphorylation by the combined action of DHP-lysine and UVA was assessed in Hs27 fibroblasts. 30 min after photosensitization cells were lysed and analyzed by Western blotting using polyclonal anti-phospho p38 and anti-total p38 antibodies as described in ‘Materials and methods’.

NIH-PA Author Manuscript

NIH-PA Author Manuscript

NIH-PA Author Manuscript

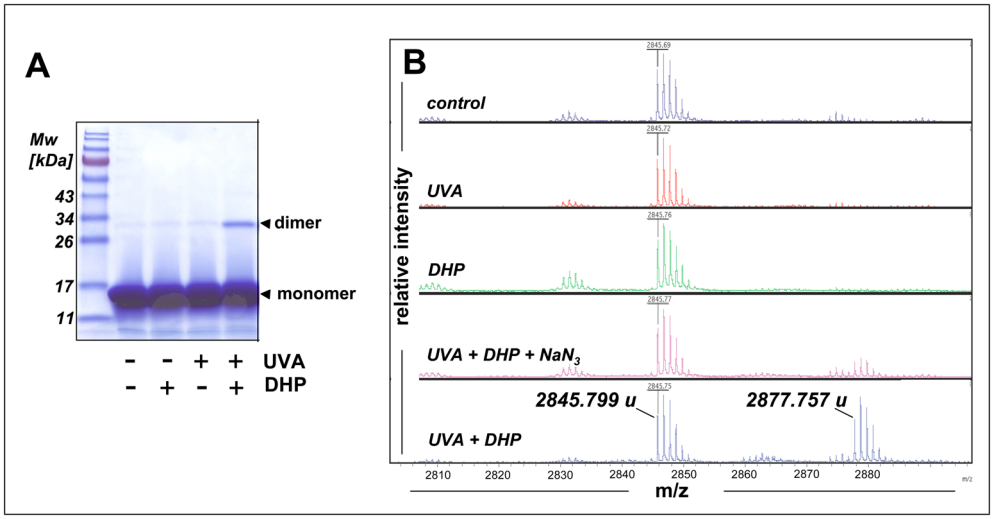

Figure 6. Induction and antioxidant modulation of protein and peptide photodamage sensitized by DHP-lysine

(A) Photosensitization of protein damage by DHP-lysine was assessed using an RNAse A photo-crosslinking assay. RNAse A (10 mg/mL PBS) was irradiated with UVA (9.9 J/cm^2) in the absence or presence of DHP-lysine (50 μM) and a reaction aliquot was analyzed by 15% SDS-PAGE followed by Coomassie-staining [Migration positions of molecular weight standard (Mw), RNAse monomer, and RNAse dimer are indicated]. (B) Mass spectrometric analysis of peptide photooxidation sensitized by DHP-lysine. The peptide melittin (1 mg/mL PBS) was UVA-irradiated (9.9 J/cm^2 UVA) in the presence or absence of DHP-lysine (10 μM) followed by MALDI-TOF mass spectrometric analysis. In an additional group, exposure to UVA plus DHP-lysine occurred in the presence of NaN_3 (10 mM). Monoisotopic mass peaks are indicated.

NIH-PA Author Manuscript

NIH-PA Author Manuscript

NIH-PA Author Manuscript

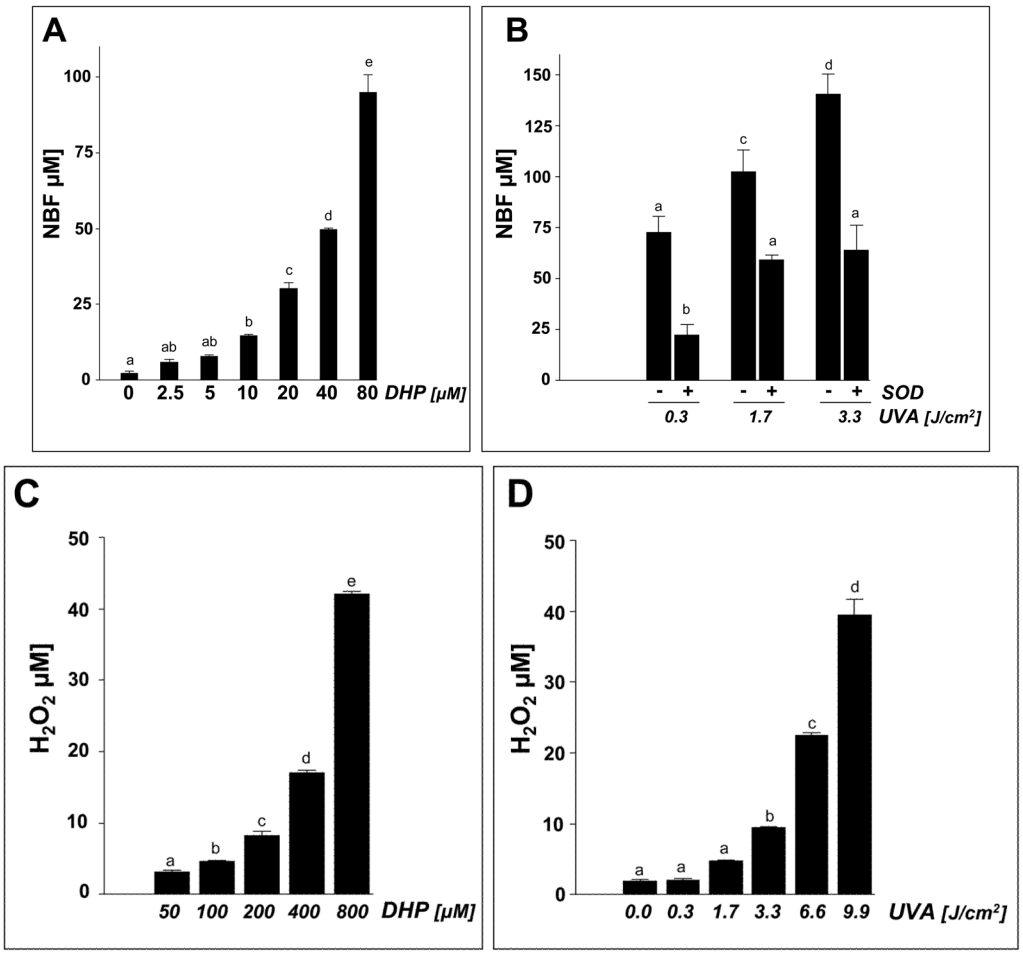

NIH-PA Author Manuscript

NIH-PA Author Manuscript

NIH-PA Author Manuscript

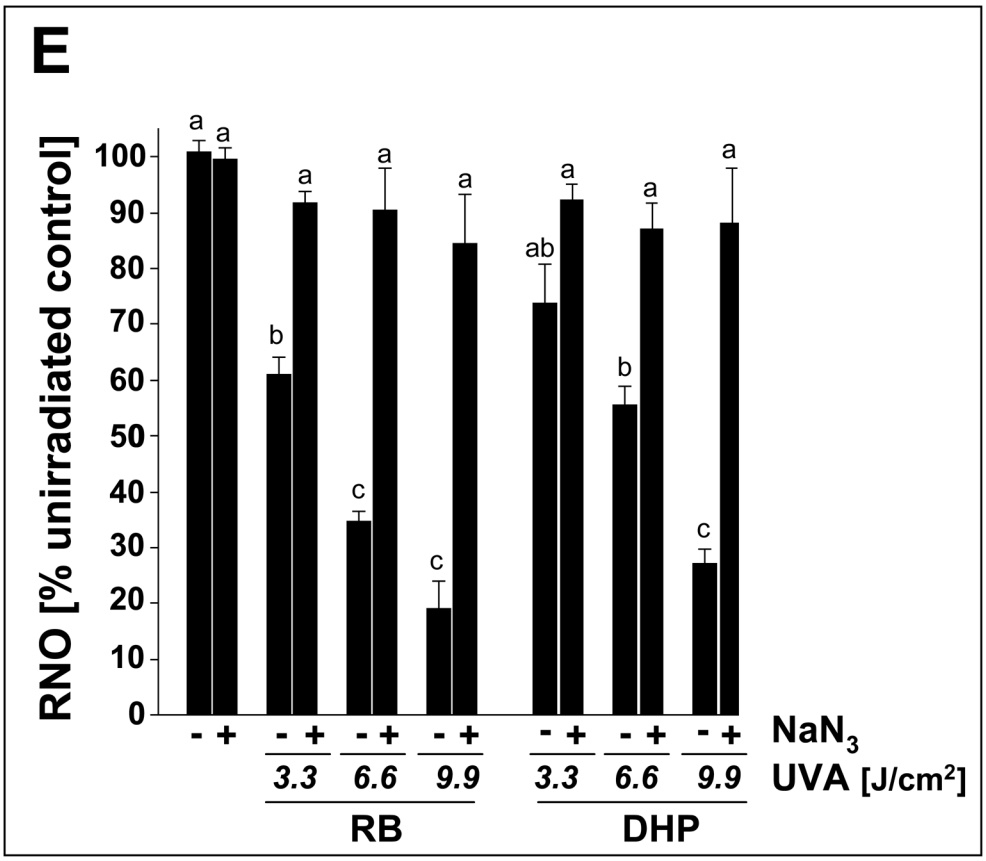

Fig. 7. DHP-lysine-sensitized production of ROS

Photosensitization of ROS formation upon exposure to UVA was examined over a wide concentration range of DHP-lysine (2.5 up to 800 μM). (A) DHP-lysine-sensitized NBT reduction measured by NBF generation as a function of DHP-lysine concentration (3.3 J/cm^2 UVA). (B) SOD-suppressible NBF formation indicative of superoxide formation was assessed by exposing DHP-lysine (100 μM) to increasing doses of UVA in the presence or absence of SOD (15000 u/mL). Values represent the mean of three independent experiments + SD. (C) Dose response of H_2O_2 production as a function of DHP- lysine concentration (9.9 J/cm^2 UVA). (D) Dose response of H_2O_2 production as a function of UVA dose (800 μM DHP-lysine). (E) Singlet oxygen formation as evidenced by the RNO bleaching assay. Loss of RNO absorbance resulting from photosensitization by Rose Bengal (RB, 1 μM) and DHP-lysine (20 μM) was examined as a function of UVA dose in the absence or presence of NaN_3 (10 mM).

NIH-PA Author Manuscript

NIH-PA Author Manuscript

NIH-PA Author Manuscript

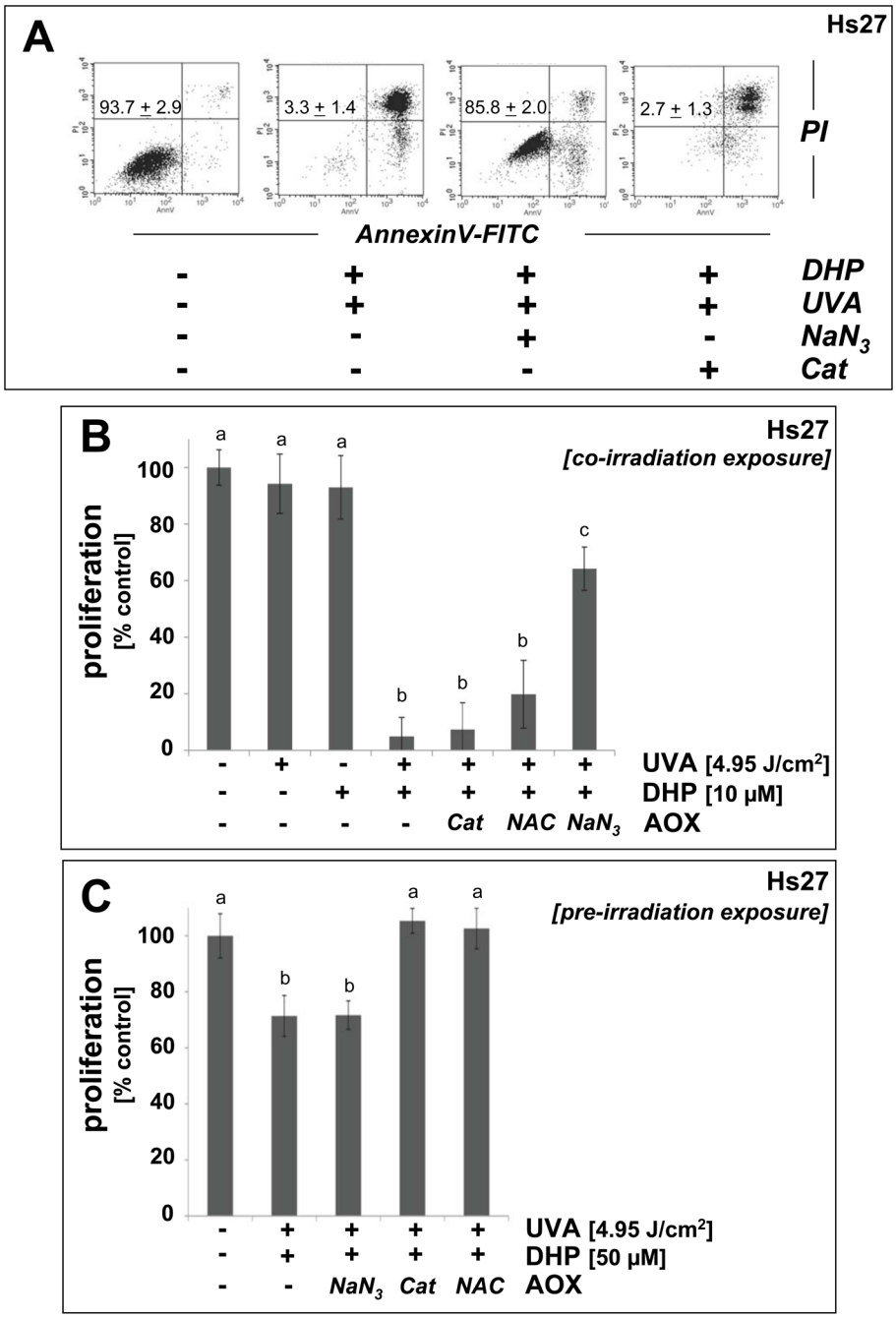

Fig. 8. Antioxidant protection of human skin fibroblasts against DHP-lysine phototoxicity

(A) Human Hs27 fibroblasts were exposed to the combined action ('co-irradiation exposure') of UVA-irradiation (9.9 J/cm^2) and DHP-lysine (50 μM) in the presence or absence of various antioxidants including NaN_3 (10 mM) and catalase (Cat, 400 u/mL). Viability was examined 24 h after exposure by flow cytometric analysis of annexinV-FITC/PI-stained cells. (B) Cells were exposed to the combined action of UVA-irradiation (4.95 J/cm^2) and DHP-lysine (10 μM) in the presence or absence of various antioxidants including NaN_3 (10 mM), NAC (10 mM), and catalase (Cat, 400 u/mL). Proliferation was examined 72 h after exposure as specified in Materials and Methods. (C) DHP-lysine (10 μM) was exposed to UVA (9.9 J/cm^2) ('pre-irradiation exposure') and then immediately added to un-

irradiated cells in the presence or absence of various antioxidants (30 min exposure, followed by media change), and proliferation was examined 72 h later.

NIH-PA Author Manuscript
NIH-PA Author Manuscript
NIH-PA Author Manuscript